Available online at www.sciencedirect.com
ScienceDirect
Journal of Crystal Growth 297 (2006) 390–395
JOURNAL OF CRYSTAL GROWTH
www.elsevier.com/locate/jcrysgro

Effect of carbon and post-annealing treatment on magnetic properties of high-quality iron thin films

Kewei Liu[a,b], Dezhen Shen[a], Jiying Zhang[a,*], Xiaojie Wu[a,b], Binghui Li[a], Bingsheng Li[a], Youming Lu[a], Xiwu Fan[a]

[a]*Key Laboratory of Excited State Processes, Changchun Insititute of Optics, Fine Mechanics and Physics, Chinese Academy of Sciences, Changchun 130033, PR China*
[b]*Graduate School of the Chinese Academy of Sciences, Beijing 100049, PR China*

Received 13 August 2006; received in revised form 27 September 2006; accepted 6 October 2006
Communicated by R. Fornari
Available online 28 November 2006

Abstract

High-quality (1 1 0) Fe films with thickness of 200 nm were grown on Al_2O_3 (0 0 0 6) substrates by low-pressure metal organic chemical vapor deposition (LP-MOCVD). The effects of residual carbon and post-annealing treatment on magnetic properties of Fe films were studied. X-ray photoelectron spectroscopy (XPS) measurements revealed that almost all the interstitial carbon atoms in Fe films can be removed by annealing at temperature of 600 °C. Vibrating sample magnetometer (VSM) showed that the in-plane (out-of-plane) coercivity of the film annealed at 600 °C is clearly larger (smaller) than that of as-grown one, which can be assigned to the tensile stress relaxation due to the removal of carbon. As the annealing temperature increased from 600 to 750 °C, the in-plane coercivity decreased while the out-of-plane coercivity increased. Meanwhile, the in-plane remanence ratios increased rapidly with the increase of annealing temperature, but the out-of-plane remanence ratios changed slightly. The origin of the changes of magnetic properties with annealing temperatures was discussed.

PACS: 75.20.En; 75.30.Gw; 75.50.Bb; 75.70.Ak

Keywords: A1. Magnetic fields; A1. Stresses; A3. Low pressure metalorganic vapor phase epitaxy; B1. Metals; B2. Magnetic materials; Fe film

1. Introduction

Magnetic films grown on different substrates have attracted much attention due to their broad applications in modern technologies such as write heads, magnetoresistive sensors, magnetic thin film inductors and microelectromechanical systems. Recently, iron films are subject of intense research work and there are many reports on the epitaxial growth and magnetic properties of Fe films [1–6]. Up to now, most of Fe films were deposited by molecular beam epitaxy (MBE) [18–23] and various materials (semiconductors, metals and insulators) have been selected as substrates due to their specific properties, such as lattice match, crystalline quality, thermal stability, etc. [7–17]

For the magnetic properties, Shiratsuchi et al. [17] have investigated the effect of substrate inclination on the in-plane magnetic anisotropy of ultrathin Fe films grown on Al_2O_3 (0 0 0 1) using MBE. For Fe films grown on flat Al_2O_3 substrates, no preferred direction of magnetization exists in the film plane due to the three equivalent epitaxial orientations of Fe (1 1 0) that form. However, for Fe grown on an inclined Al_2O_3 substrate, a uniaxial anisotropy appears that is parallel to the step edges. Swerts et al. [19] reported the influence of surface roughness on the coercivity of Fe thin films. The evolution of the magnetic anisotropy as a function of Fe-deposited thickness is very well described as a result of competition between

*Corresponding author. Key Laboratory of Excited State Processes, Changchun Insititute of Optics, Fine Mechanics and Physics, Chinese Academy of Sciences, Changchun 130033, PR China.
E-mail address: zhangjy53@yahoo.com.cn (J.Y. Zhang).

0022-0248/$ - see front matter © 2006 Elsevier B.V. All rights reserved.
doi:10.1016/j.jcrysgro.2006.10.148

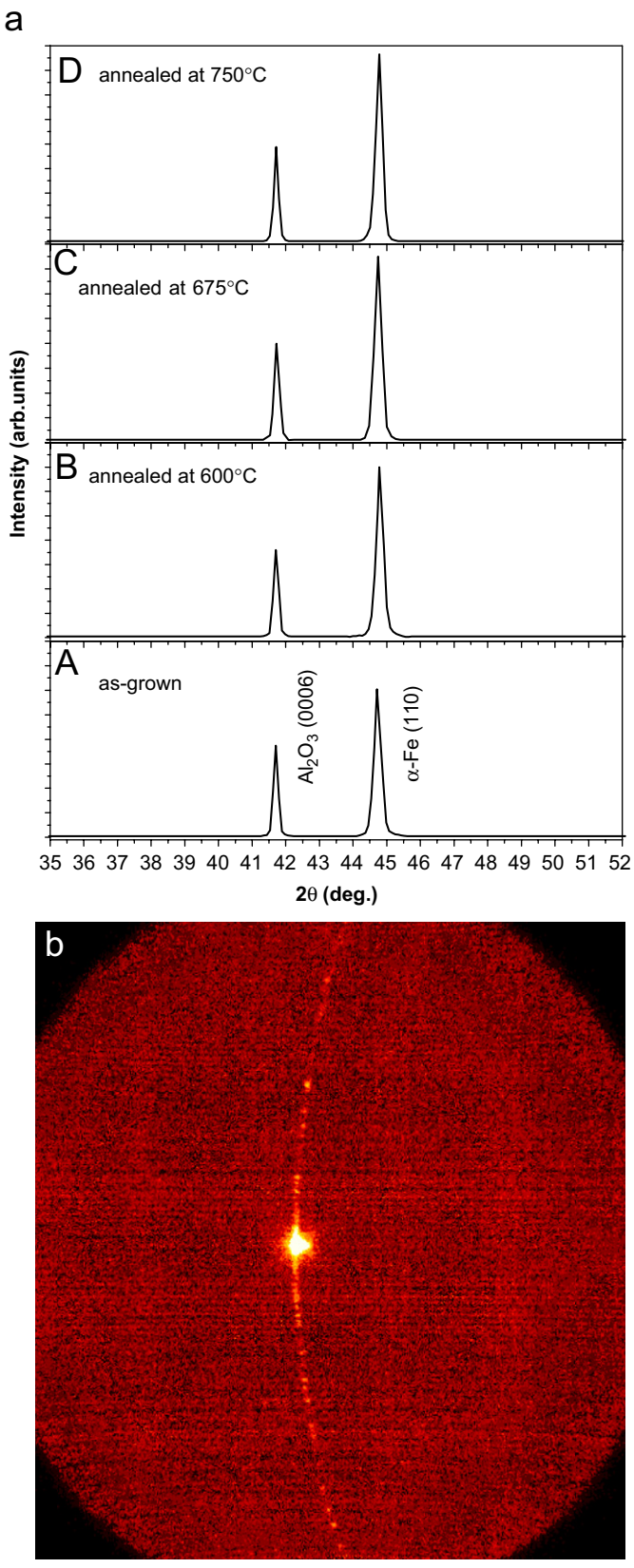

Fig. 1. (a) XRD spectra of the as-grown sample (A) and the samples annealed at 600 °C (B), 675 °C (C) and 750 °C (D). (b) GADDS image of the as-grown Fe film. scanned from 43° to 47°.

magnetoelastic (ME) coupling and interface uniaxial magnetic anisotropy (UMA) [5]. Meanwhile, the structural properties and the relationship between Fe film and substrate were also studied broadly.

However, only little information can be found for Fe films fabricated by MOCVD. In 1982, Kaplan firstly prepared Fe films on GaAs (1 0 0) by MOCVD using ironpentacarbonyl ($Fe(CO)_5$) as source. These films yielded ferromagnetic resonance lines having widths comparable to those observed for Fe whiskers, and approaching those of MBE-grown samples [30]. More recently, Haugan et al. [24] found that single-crystal Fe films can be grown on (1 1 0) GaAs substrates at the temperature ranging from 200 to 330 °C by MOCVD, and Fe films (>20 nm) were ferromagnetic with the in-plane easy axis along the [1 1 0] direction. Our previous work has also studied the growth and magnetic properties of Fe films on GaAs [31] and sapphire [32] by low-pressure metal organic chemical vapor deposition (LP-MOCVD) using different processes.

According to the reports, it can be noted that the magnetic properties of magnetic films are sensitive to impurities (C, S, O, P, N), preparation methods, microstructure (grain size, porosity and stress), deposition conditions (temperature, pressure) and post-annealing treatment [20,25–28]. And it is unavoidable that the Fe films deposited by MOCVD using $Fe(CO)_5$ as the material source usually contain a little carbon. However, to our knowledge, no study about the effect of carbon on magnetic properties for iron films prepared by MOCVD has been performed.

In this paper, high-quality Fe films have been prepared by LP-MOCVD. The sapphires with (0 0 0 6) orientation were used as substrates due to the high thermal stability. After the deposition, the samples were annealed at different temperatures in hydrogen atmosphere. The carbon content and magnetic properties of the Fe films have been studied before and after annealing.

2. Experiment

Fe films were grown on (0 0 0 6) sapphire substrate by a LP-MOCVD system with a horizontal rectangular quartz reactor. The $Fe(CO)_5$ with hydrogen as carrying gas was used as the Fe source. The source was kept at 10 °C during the deposition. The semi-insulating sapphires with (0 0 0 6) orientation were used as substrates. Before deposition, the substrates were cleaned by acetone and ethanol for 5 min in an ultrasonic bath and etched in an acid solution ($3H_2SO_4 + 1H_3PO_4$) for 5 min at 160 °C, followed by a de-ionized water rinse. The growth was performed at 320 °C with the pressure of 150 Torr. The flow rate of H_2/$Fe(CO)_5$ bubbler was kept at 10 ml/min and the total H_2 gas flow is 1400 ml/min. The growth rate is 6.5 nm/min and the thickness of the films is approximately 200 nm. After the growth, the samples were treated in hydrogen atmosphere for 30 min with the atmosphere pressure at the temperatures of 600, 675 and 750 °C, respectively.

The content of carbon in Fe films was calculated by energy-dispersive spectroscopy (EDS). The crystal structure and the d-spacing lattice constant were investigated by X-ray diffraction (XRD). As for magnetic properties of the films, M–H curves were measured with a vibrating sample magnetometer (VSM) at room temperature.

3. Results and discussions

A Ringaku O/max-RA X-ray diffractometer with Cu Kα radiation ($\lambda = 0.154178$ nm) was used to make $\theta-2\theta$ scans to evaluate the crystalline property and determine the (1 1 0) d-spacing lattice constant of the Fe films. Fig. 1(a) shows the XRD spectra of the as-grown sample (A) and the samples annealed at 600 (B), 675 (C) and 750 °C (D). Besides the (0 0 0 6) diffraction peak of the Al_2O_3 substrate, there is only one intense diffraction peak appearing in the spectra, which can be attributed to the α-Fe (1 1 0) diffraction pattern. In Fig. 1(a), we noticed that the (1 1 0) diffraction peaks for all the films have strong intensities and small full-width at half-maximum (FWHM). In order to further confirm the crystal quality of the Fe films, general area diffraction detector system (GADDS) was selected to evaluate the as-grown samples, as shown in Fig. 1(b). In this figure, only one light spot can be seen, which indicates that our Fe thin film is preferentially oriented out of plane. According to the XRD results, it can be concluded that high-quality Fe epitaxial layer has been grown on (0 0 0 6) Al_2O_3 substrates by LP-MOCVD system, although there is a large lattice mismatch between Fe (1 1 0) and Al_2O_3 (0 0 0 6). In addition, it can be seen from Fig. 1(a) that the diffraction peaks of Fe (1 1 0) shifted to high angles side after annealing at 600 °C, but do not show much significant change with the annealing temperature increasing from 600 to 750 °C. Fig. 2(a) shows the variation of (1 1 0) d-spacing lattice constants obtained from the XRD patterns in Fig. 1(a). The derived (1 1 0) d-spacing lattice constants for all the three post-annealed Fe films were smaller than that of as-grown one and slightly increased with the annealing temperature increasing from 600 to 750 °C. The carbon contents in Fe films were calculated by EDS patterns before and after annealing. An atomic ratio of carbon is ~1.2% for the as-grown sample. But after annealed at 600, 675 and 750 °C, the carbon has been removed entirely. It is well known that C, S, O and N usually act as interstitial atoms in iron materials. Fig. 2(b) showed the schematic representation of a C-filled octahedral interstice in bcc Fe. The octahedral site is formed by six Fe atoms. Four atoms are situated in a {1 0 0} plane at a distance $a/\sqrt{2}$ from the center of the octahedral and two Fe atoms at a distance $a/2$ on an ⟨1 0 0⟩ axis perpendicular to the {1 0 0} plane. These octahedral interstices ($\Delta = a-2r_{Fe} = 0.03455$ nm) are smaller than the diameter of carbon atom ($d = 0.154$ nm). So the existence of interstitial carbon atoms could induce the lattice expansion in bcc Fe crystal lattice. Therefore, the removal of carbon in films by annealing could be responsible for the change of (1 1 0) d-spacing lattice constants of the as-grown sample and the 600 °C annealed one. In addition, the slightly increase of the (1 1 0) d-spacing lattice constants with the annealing temperature increasing from 600 to 750 °C can be explained by the stress relaxation. On the other hand, the (1 1 0) d-spacing lattice constants for both as-prepared and post-annealed samples are smaller than that of bulk α-Fe (0.20269 nm). It may be caused by the stress including compressive stress (existing in out-of-plane) and tensile stress (existing in in-plane) due to the large lattice mismatch between Fe films and substrates. A possible schematic diagram of the crystal structure for the Fe/Al_2O_3 heterostructure, taking into account for the stress effect is shown in Fig. 3. The epitaxial relationship indicated that the (1 1 0) orientation of Fe is perpendicular to the surface of Al_2O_3. According to this figure, a_{Fe} (0.28665 nm) is smaller than $a_{Al_2O_3}$ (0.4759 nm) and the in-plane lattice mismatch between Fe and Al_2O_3 is 39.76%. Therefore, the stress effect occurred between Fe film and sapphire, which could well explain the little decrease of the (1 1 0) d-spacing lattice constants of Fe compared with the bulk α-Fe.

Fig. 4 showed X-ray photoelectron spectroscopy (XPS) spectra of the as-grown sample and the sample annealed at 600 °C. The surface of the samples was cleaned with 3 keV Ar^+ for 5 min before detection. In Fig. 4(a), the binding energy peaks situated at 707 and 720 eV can be attributed to $Fe_{2p3/2}$ and $Fe_{2p1/2}$ of pure Fe, and there is almost no energy difference of Fe_{2p} between the as-grown and 600 °C annealing sample. The XPS spectra of C_{1s} were presented in Fig. 4(b) for the as-grown (solid line) and the sample annealed at 600 °C (dotted line). The peaks at 288 eV is evidently independent of annealing and it could be attributed to adventitious carbon dioxide. It is noted that the peak at 284.6 eV, which is related to pure carbon disappeared after annealing at 600 °C. This change is in good agreement with the results of EDS. Additionally, no other phase like cementite was observed in our research.

The magnetic properties of Fe films were studied with a VSM. The in-plane and out-of-plane field-dependent magnetization measurements of the samples were carried out at room temperature. Fig. 5(a) and (b) showed the in-plane and out-of-plane magnetic hysteresis loops of the as-grown and the annealed Fe samples, respectively. All samples have no preferred directions of in-plane magnetization due to the three equivalent variants of the epitaxial Fe (1 1 0) on Al_2O_3 (0 0 0 6), which is in coincidence with the results of Shiratsuchi et al. [17] For the as-grown sample, it can be seen that the in-plane hysteresis loop has lower coercivity (H_c) and higher remanence ratio (M_r/M_s) than that of out-of-plane. Furthermore, the in-plane hysteresis loops approach the saturation point faster than the out-of-plane. According to these results, it is concluded that the as-grown Fe films are ferromagnetic with easy axis along the film surface. However, after annealing at 600 °C, the out-of-plane hysteresis loop has lower coercivity (H_c) and higher remanence ratio (M_r/M_s) than that of in-plane.

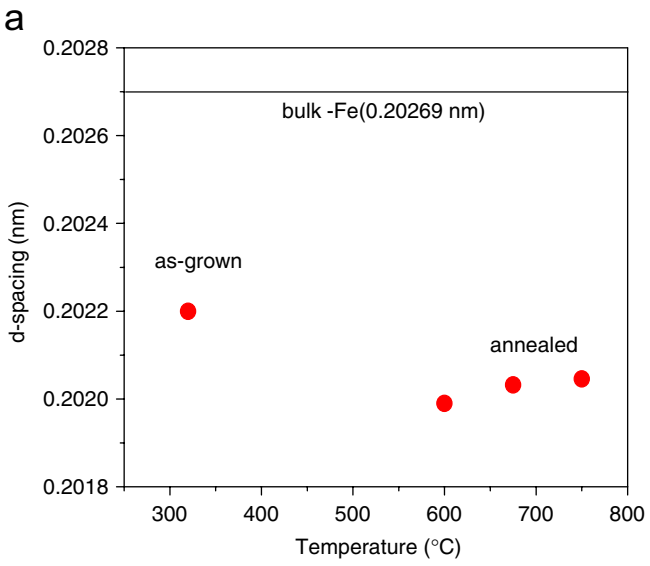

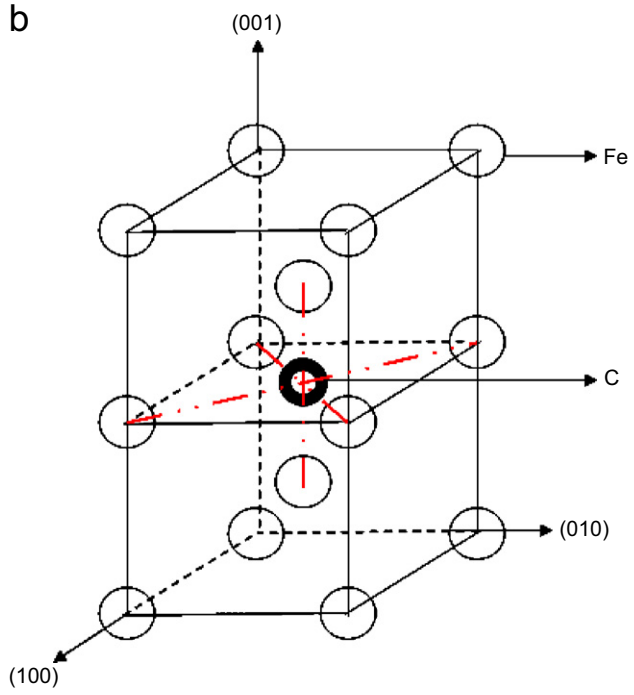

Fig. 2. (a) (1 1 0) d-spacing lattice constant vs. temperature; (b)schematic representation of a C-filled octahedral interstice in bcc Fe.

According to EDS and XPS results, the carbon atoms were taken away after annealing at 600 °C. Therefore, the remarkable change of magnetic properties between the as-grown and the 600 °C annealed samples can be attributed to the removal of the carbon atoms and the 600 °C thermal treatment. However, the effect of thermal treatment at different temperatures on magnetic properties (Fig. 6) showed a different trend with increasing the annealing temperature. So the effect of 600°C thermal treatment on the difference of magnetic properties between the as-grown and the 600°C annealed samples can be excluded. According to Fig. 2(b), C-filling in octahedral interstices could lead to a remarkable lattice expansion

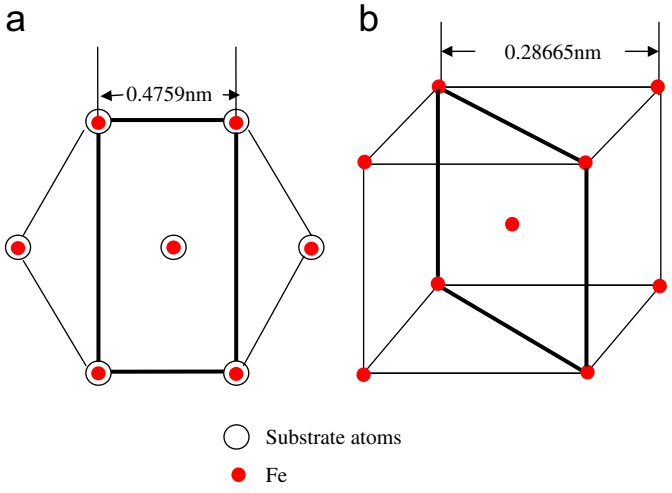

Fig. 3. (a) Crystallographic relation between Fe(1 1 0) and Al_2O_3 (0 0 0 1) substrate, (b) the structure of (bcc) Fe.

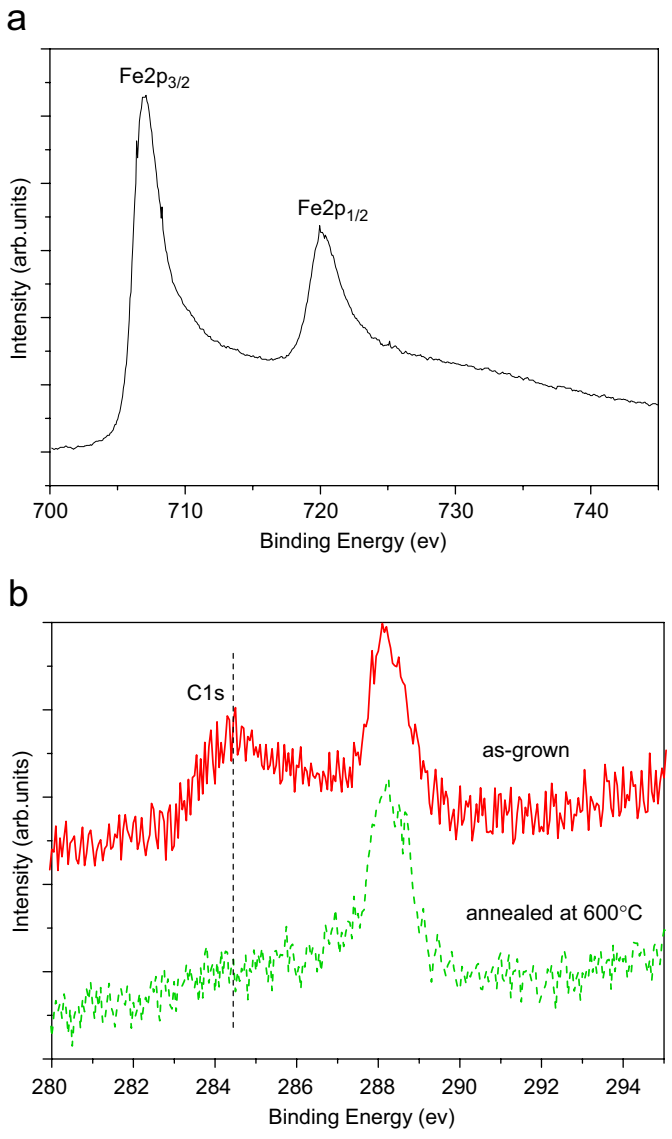

Fig. 4. XPS spectra of Fe_{2p} (a) and C_{1s} (b) for the as-grown and the 600 °C annealed samples.

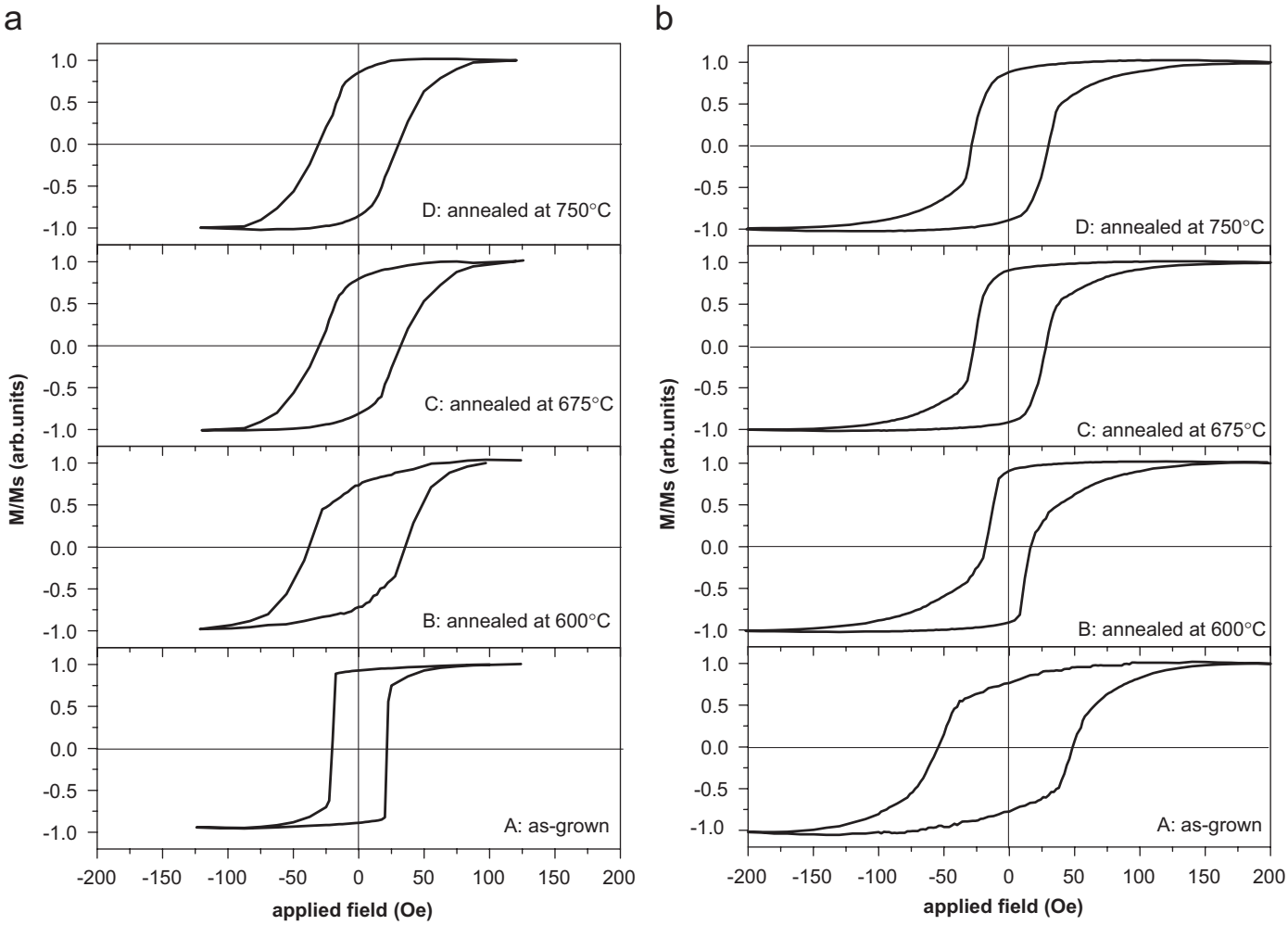

Fig. 5. Magnetization vs. applied field: (a) parallel and (b) perpendicular to the surface of Fe films.

effect and tensile stress. This stress strongly effect on magnetic properties of Fe films [26]. Furthermore, as interstitial atoms, the carbon in iron films could modify the distribution of the magnetic domain and domain wall. Therefore, the magnetic properties of the Fe films before and after annealing at 600 °C have large difference due to the removal of the carbon atoms.

Fig. 6(a) and (b) showed the variation of the coercivities and remanence ratios with annealing temperatures. In Fig. 6(a), as the annealing temperature increased from 600 to 750 °C, the in-plane coercivity decreased gradually, while the out-of-plane coercivity showed a completely different way of change compared with that of the in-plane. It is well known that the coercivity is determined not only by the microstructure (grain size, porosity, stress) affected by the deposition parameters [25,28], but also by the crystal quality and impurity [26]. In this work, the carbon has been removed by annealing at different temperatures. Therefore, the impacts of carbon on the magnetic properties can be excluded. On the other hand, the oxidation on the surface of the films may also induce magnetic change. However, no detectable Fe–O compound was observed in as-grown and post-annealed films in XRD pattern. Furthermore, XPS analysis did not show the peaks related to Fe^{2+} or Fe^{3+}. Moreover, shape anisotropy is not modified by annealing as the film thickness is not strongly modified during annealing. So there must be other reasons for the change of coercivity. Since the crystal lattice constant of sapphire is larger than that of Fe film, two types of stress including compressive stress (existing in out-of-plane) and tensile stress (existing in in-plane) are considered to exist in the film. So both the compressive stress (which could make the out-of-plane coercivity lower) and the tensile stress (which could make the in-plane coercivity higher) decreased with increasing annealing temperature. So the change of the coercivity in Fig. 6(a) is probably caused by the change of stress in films after annealing at different temperatures [26–28] in good agreement with the results of XRD. In Fig. 6(b), with increasing the annealing temperature from 600 to 750 °C, the out-of-plane remanence ratios changed a little, while that of the in-plane increased rapidly. After annealing at 750 °C, the remanence ratios between out-of-plane and in-plane became nearly identical. Besides the change of stress, these phenomena were probably caused by magnetocrystalline anisotropy [17,29] and interface effects [19,20].

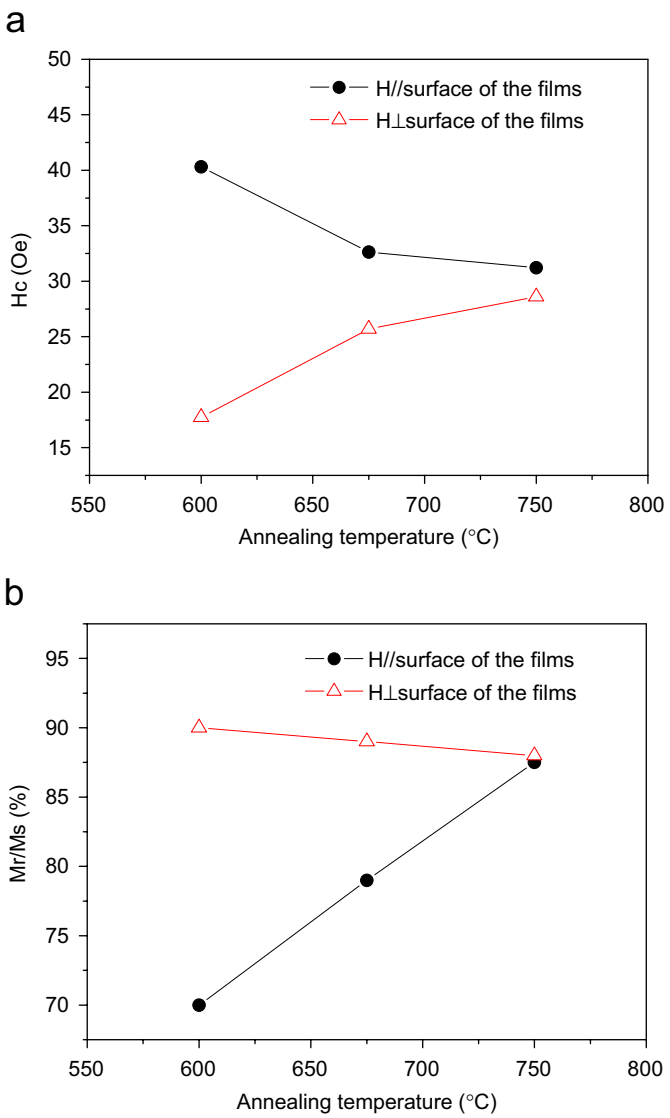

Fig. 6. The variations of the coercivity (a) and the remanence ratio (b) annealing temperatures.

4. Conclusion

Structure, composition and magnetic properties of Fe thin films were investigated as a function of annealing temperature. The carbon atoms in Fe films (~1.2%) have been remove entirely after annealing. The magnetic hysteresis loops of the 600 °C annealed sample showed the opposite behavior compared to the as-grown sample. This phenomenon can be explained by the tensile stress relaxation due to the removal of carbon. With increasing annealing temperature from 600 to 750 °C, the in-plane coercivity of the samples decreased, while the out-of-plane increased. Meanwhile, the out-of-plane remanence ratios changed slightly when we increased the annealing temperature from 600 to 750 °C, but the in-plane remanence ratios increased rapidly. The possible reason for this trend is that the change of two stress components of compressive stress (out-of-plane) and tensile stress (in-plane).

Acknowledgments

The authors would like to express their gratitude to Dr. Jiangang Ma. This work is supported by the Key Project of National Natural Science Foundation of China under Grant no. 60336020, the National Natural Science Foundation of China under Grant nos. 50402016, 60501025, 60278031 and 60506014 and the Innovation Project of Chinese Academy of Sciences.

Reference

[1] S. Datta, B. Das, Appl. Phys. Lett. 56 (1990) 665.
[2] R. Sato, K. Mizushima, Appl. Phys. Lett. 79 (2001) 1157.
[3] H.J. Zhu, et al., Phys. Rev. Lett. 87 (2001) 016601.
[4] A.T. Hanbicki, et al., Appl. Phys. Lett. 80 (2002) 1240.
[5] O. Thomas, Q. Shen, P. Schieffer, N. Tournerie, B. Le′pine, Phys. Rev. Lett. 90 (2003) 017205-1.
[6] Y. Chye, V. Huard, M.E. White, P.M. Petroff, Appl. Phys. Lett. 80 (2002) 449.
[7] J.R. Waldrop, R.W. Grant, Appl. Phys. Lett. 34 (1979) 630.
[8] G.A. Prinz, J.J. Krebs, Appl. Phys. Lett. 39 (1981) 397.
[9] G.A. Prinz, G.T. Rado, J.J. Krebs, J. Appl. Phys. 53 (1982) 2087.
[10] E.M. Kneedler, B.T. Jonker, P.M. Thibado, R.J. Wagner, B.V. Shanabrook, L.J. Whitman, Phys. Rev. B 56 (1997) 8163.
[11] J.M. Florczak, E.D. Dahlberg, Phys. Rev. B 44 (1991) 9338.
[12] C. Daboo, et al., Phys. Rev. B 51 (1995) 15964.
[13] A. Filipe, A. Schuhl, P. Galtier, Appl. Phys. Lett. 70 (1997) 129.
[14] M. Zölfl, M. Brockmann, M. Köhler, S. Kreuzer, T. Schweinböck, S. Miethaner, F. Bensch, G. Bayreuther, J. Magn. Magn. Mater. 175 (1997) 16.
[15] Y.B. Xu, E.T.M. Kernohan, D.J. Freeland, A. Ercole, M. Tselepi, J.A.C. Bland, Phys. Rev. B 58 (1998) 890.
[16] H.-P. Schönherr, R. Nötzel, W. Ma, K. Ploog, J. Appl. Pyhs. 89 (2001) 169.
[17] Y. Shiratsuchi, Y. Endo, M. Yamamoto, J. Appl. Phys. 97 (2005) 10J106.
[18] P.K. Muduli, J. Herfort, H.-P. Schönherr, K. H. Ploog, J. Appl. Phys. 97 (2005) 123904.
[19] J. Swerts, K. Temst, M.J. Van Bael, C. Van Haesendonck, Y. Bruynseraede, Appl. Phys. Lett. 82 (2003) 1239.
[20] Y. Chye, V. Huard, M.E. White, P.M. Petroff, Appl. Phys. Lett. 80 (2002) 449.
[21] X.S. Jin, C. McEvoy, I.V. Shvets, J. Appl. Phys. 97 (2005) 10M103.
[22] W. Kipferl, M. Sperl, T. Hagler, R. Meier, G. Bayreuther, J. Appl. Phys. 97 (2005) 10B313.
[23] T.A. Moore, M.J. Walker, A.S. Middleton, J.A.C. Blanda, J. Appl. Phys. 97 (2005) 053903.
[24] H.J. Haugan, B.D. McCombe, P.G. Mattocks, J. Magn. Magn. Mater. 247 (2002) 296.
[25] Y.K. Kim, M. Oliveria, J. Appl. Phys. 74(2) (1993), 15 July.
[26] A.R. Chezan_, C.B. Craus, N.G. Chechenin, T. Vystavel, L. Niesen, J.Th.M. De Hosson, D.O. Boerma, J. Magn. Magn. Mater.299 (2006) 219.
[27] D. Sander, A. Enders, J. Kirschner, J. Magn. Magn. Mater. 200 (1999) 439.
[28] S.M. Naa, S.J. Suha, H.J. Kimb, S.H. Lim, J. Magn. Magn. Mater. 239 (2002) 570.
[29] R. Moosbuhler,, F. Bensch, M. Dumm, and G. Bayreuther, J. Appl. Phys. 91(10) (2002) 8757.
[30] R. Kaplan, J. Vac. Sci. Technol. A 1 (2) (1983) 551.
[31] K.W. Liu, D.Z. Shen, J.Y. Zhang, X.J. Wu, B.H. Li, B.S. Li, Y.M. Lu, X.W. Fan, Solid-State Commun. 140 (2006) 33.
[32] K.W. Liu, D.Z. Shen, J.Y. Zhang, B.S. Li, X.J. Wu, Q.J. Feng, Y.M. Lu, X.W. Fan, J. Magn. Magn. Mater. 303 (2006) 79.